Chapter 3

Observations

3.1 The Observing System

All the observations were made with the 10.4m millimeter wave radio telescope at the Raman Research Institute campus at Bangalore (longitude: 77° 35'; latitude: 13° 01'N; 930m above mean sea level.) The observing system used lias been described in some detail by Patel(1990). We give a brief description here. Figure 3.1(a) shows the telescope. A schematic diagram of the system is shown in figure 3.1(b). Tlie telescope has an altitude-azimuth mount with the receiver at the Nasmyth focus. The primary is a 10.4m paraboloid made from hexagonal honeycomb sandwiched aluminium panels, with a surface accuracy of $\sim 100\mu$ rms. Tlre secondary is a hyperboloid of diameter 60cms and eccentricity 1.06. The tertiary mirror can be switched to throw tlie beam a few arcminutes. The receiver is a 20K cooled Schottky mixer type with 1.5 GHz IF. Tlie IF output is further down converted to 400 MHz before being fed to tlie backencls. The backends in use are a 256 channel filterbank with 250 kHz resolution and a 500 channel acousto-optic spectrometer (AOS) with 50 kHz resolution.

3.2 Observing Method

All the CG observations were carried out in the *frequency switched mode* for three reasons. (i) Some of the CGs are bigger than the beam throw available in the beam switching system. The largest CG (CG 22) lias a size of $\sim 5'$. The beam switching system can give a maximum beam throw of only 160"; (ii) Tlie system is not stable enough to allow position switching; (iii) Frequency switching makes best use of tlie available time and is the only method possible for extended sources; the other two methods waste at least half the time looking at source-free positions, even if possible. In frequency switching the line from the source is received in different parts of the receiver pass band during alternate switching periods. This means that no time is wasted. But because between successive switching periods the receiver characteristics arc. changed (by re-tuning) the subtraction between tlie ON and OFF spectra will not be esact leading to curved baselines. Since we are not looking for low level extentled spectral features, baseline curvature is not a serious handicap in this case. A frequency offset of 15.25 MHz was used between the ON and OFF frequencies, this being the period of the baseline ripple. This choice recluced considerably the ripple in tlie final spectra requiring only polynomial fits to remove baselines. A typical baseline is shown in figure 3.2, along with a fourth order polynomial fit. The two spectral features seen arc from the ON and OFF frequency

Figure 3.1 (a): The 10.4-meter millimeter-wave radio telescope at the Raman Research Institute campus, Bangalore.

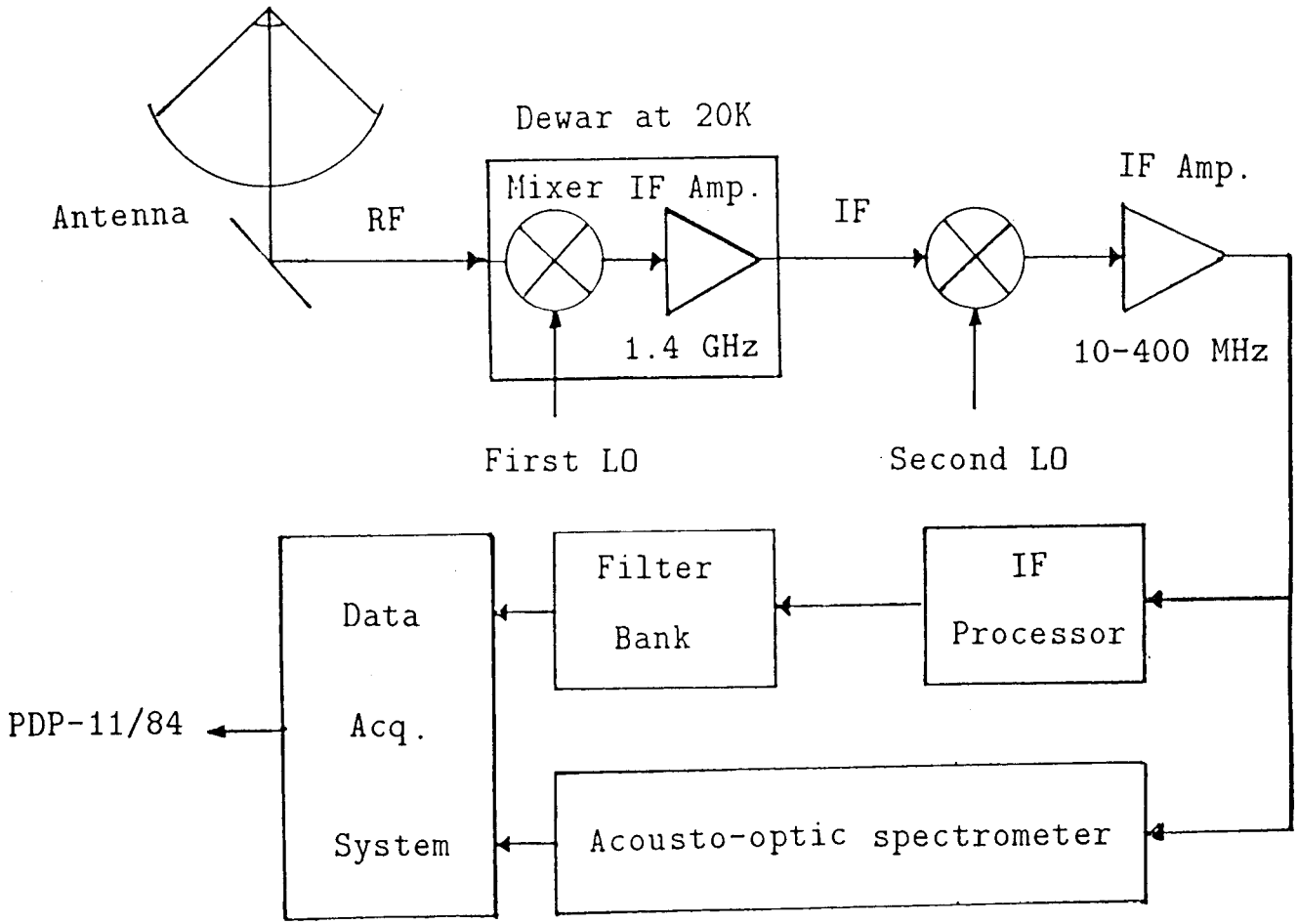

Figure 3.1 (b): A simplified block diagram of the receiver system at the 10.4m telescope.

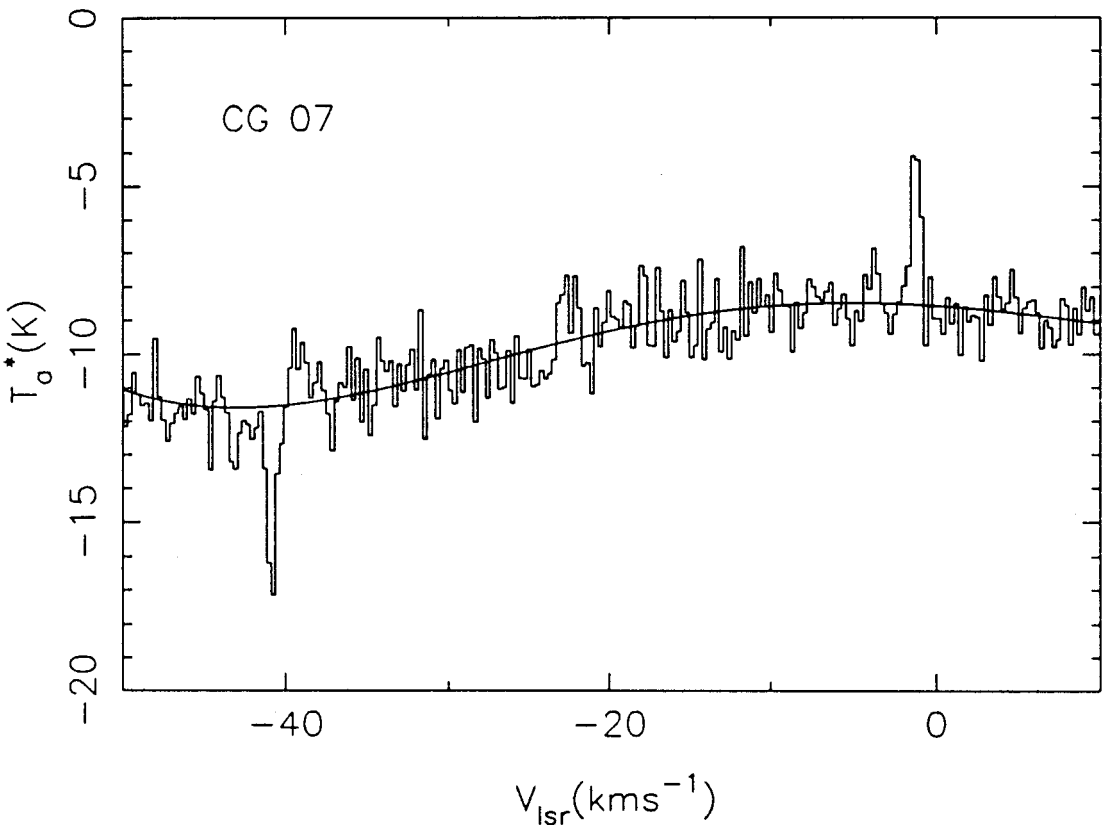

Figure 3.2: A typical baseline obtained with frequency switching. The positive and negative spectral lines of ^{12}CO are from the ON and OFF frequency observations. A fourth order polynomial fit is also shown.

observations. This spectrum is shifted, inverted and averaged with tlie unshifted to get full S/N in the final spectrum.

The switching rate was 2 Hz. Calibration was done using an ambient temperature chopper at intervals of several minutes. During the observations the atmospheric optical depth at zenith was typically 0.2. measured by telescope tipping. A11 tlie observations were carried out at elevations ranging froni 25 to 40 deg. Pointing was checked by observing Jupiter in the beam switched mode, by a procedure described by Patel(1990). Even though Jupiter covers only a specific track in tlie sky, the pointing model itself has been found to be applicable to all parts of tlie sky from observations of SiO masers. The pointing errors during the observations were less than 20″ with the rms being 6″. Figure 3.3 shows the distribution of tlie pointing errors. All the data interpreted in this thesis were obtained during 1990-91 using an AOS with 50 kHz resolution as back-elid. The data froni this AOS was later bunched to get 100 kHz resolution spectra giving a velocity resolution of 0.26 kms^{-1}. The frequency stability arid resolution of the AOS was checked by injecting a CW before observation every clay. In addition, the head of CG22 was observed several times spread over two months to get an estimate on the overall error in velocity measurements. A histograni of the distribution of errors is shown of figure 3.4. *The rms of this distribution is 0.15 kms^{-1} and we regard this number as the error on* ***all*** *velocity measurements reported in this thesis.* Ttie telluric CO line was seen in many spectra. It was easy to identify these lines froni the fact that the telluric lines always appear at an LSR velocity equal to the negative of tlie LSR correction applied.

3.3 The 1989 run

The co-ordinates for the CGs in the Gum Nebula have been listed by various authors (Hawardeen and Brand 1976; Sandqvist 1976: Zealey *et al.* 1983; Reipurth 1983). Hartley *et al.*(1986) and Feitzinger and Stuwe(1984) have noted many of tlie CGs in their catalogues of dark clouds and globules found from the SERC plates and the ESO B plates, respectively. However, a comparison of co-ordinates listed by the various authors showed inconsistencies. The Z83 co-ordinates were sometimes found to have large errors (as much as 25′ for CG2). Whenever there was disagreement we used those values which agreed with more than one list. In cases where only 283 or one more author listed co-ordinates, values from ZS3 were used. Using these criteria 27 CGs were observed during 1989. Frequency switching by 16 MHz was used. An ambient-temperature chopper-wheel was used for calibration. The back-end was an acousto-optic spectrometer with 216 kHz resolution and 120 MHz coverage. Pointing

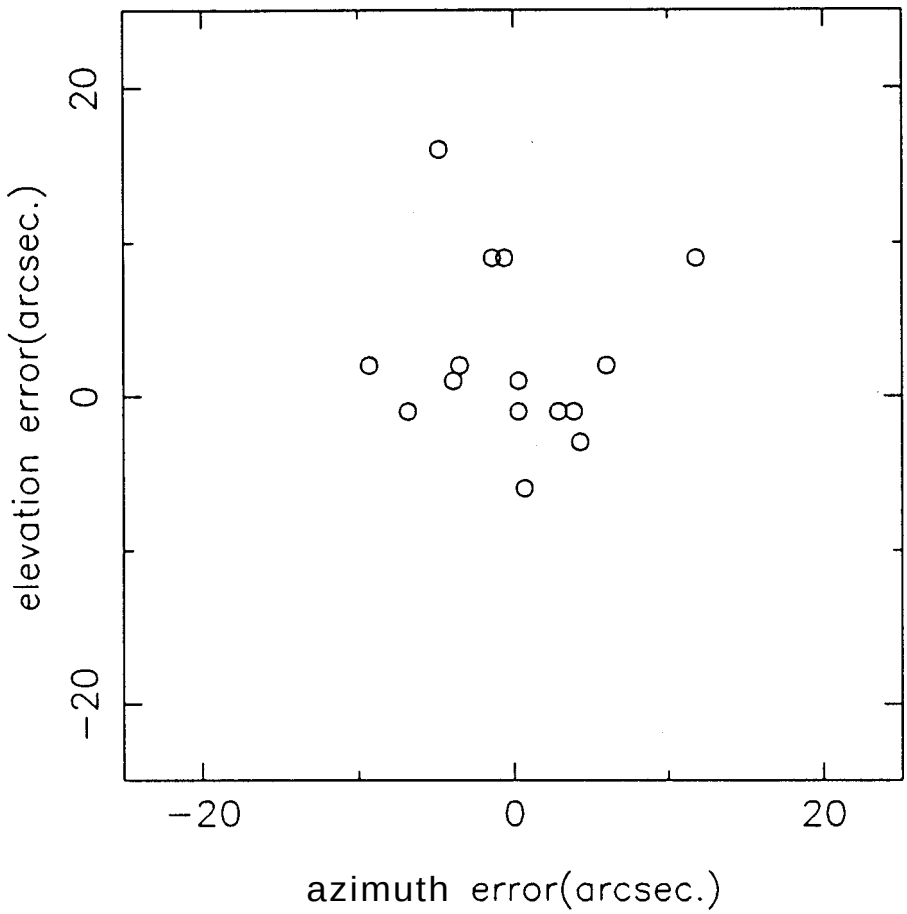

Figure **3.3:** Distribution of pointing errors measured on Jupiter.

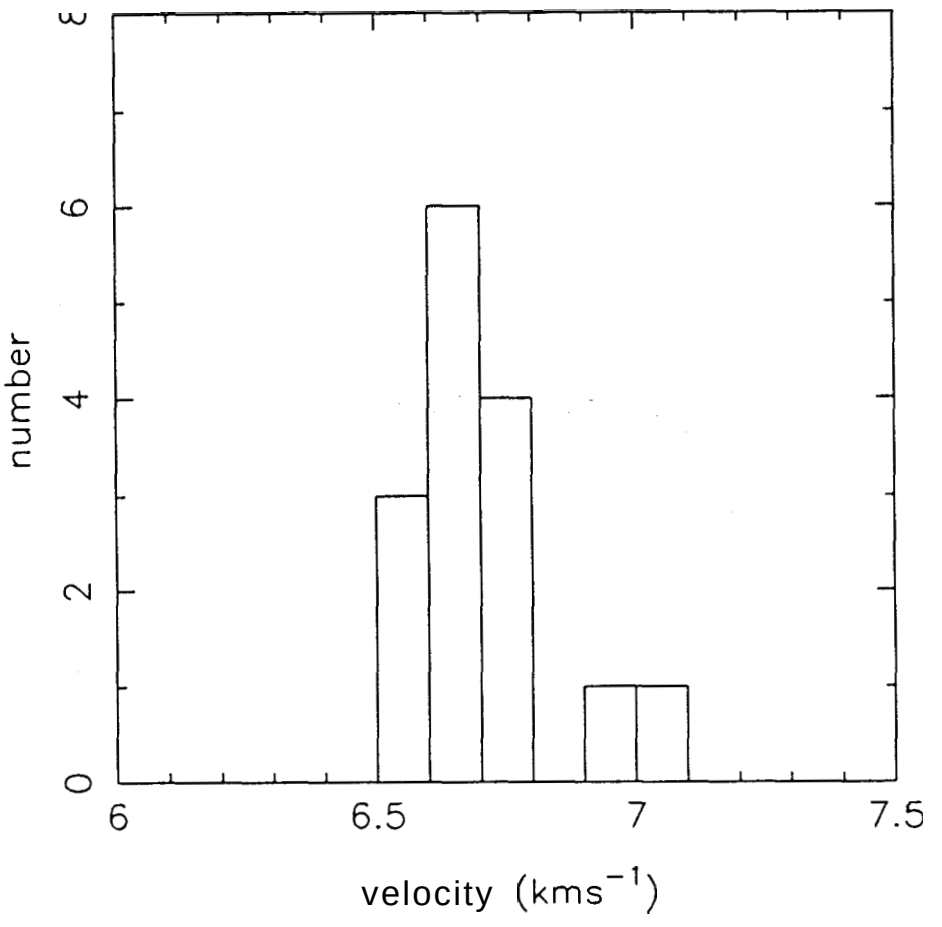

Figure 3.4: Histogram showing the distribution of the velocities measured for the head of CG22 over two months. The velocities were obtained by fitting gaussians to the lines. The rms of the distribution is 0.15 kms^{-1}.

acousto-optic spectrometer with 216 kHz resolution and 120 MHz coverage. Pointing was checked by continuum scans on Jupiter (See Patel, 1990 for details). Fourth order polynomials were fitted to remove baseline curvature. A sample spectrum is shown in figure 3.5. The noise levels and measured antenna temperatures are given in Table 3.1. Only 18 out of the 29 CGs could he detected. This was surprising because the 1′ beam of the telescope is ideally suited for detecting the CGs. It was therefore suspected that co-ordinate errors could he the cause for non-detections, especially in view of the disagreement between the different catalogs. So it was decided to remeasure tlie co-ordinates for all the CG heads and their tails from the ESO plates.

3.4 New co-ordinates

The co-ordinates of the CGs were measured from contact prints of ESO plates by relatively crude methods using magnifiers and graph sheets. The plate parameters were derived using a few known stars (listed in the SAO catalog 1966) which were used to estimate the co-ordinates for the heads and tail-ends of CGs. The errors on these measurements (estimated by leaving out one star at a time from the set used to estimate plate parameters and comparing the co-ordinate estimated for this star to its co-ordinate listed in the SAO catalog) are less than 10″. CG17, CG18, CG23 and CG34, however, could riot be located in these plates. The new measured co-ordinates of the head and tail-ends along with the tail lengths are listed in Table 3.2. Tlie co-ordinates listed are largely from our measurements. For sorne CGs and the Gum Dark Clouds (GDCs, Reipurth 1983) the co-ordinates are from published literature as mentioned in the table. CG32 seems to have two components which are listed as CG32A and B. We have listed tlie individual blobs in CG22 as seperate CGs. The measured co-ordinates show significant differences from those reported earlier. The distribution of these errors is shown is figure 3.6.

3.5 1990-91 run

During 1990-1991 a second run of ^{12}CO observations was carried out using tlie new co-ordinates. In addition to tlie heads, a few points along tlie tails were observed. All the CGs, except CG23 and CG34, were now detected. Tlie observation procedure was the same as before, except that tlie back-end used was an AOS with 50 kHz resolution arid 30 MHz coverage. A sample spectrum is shown in figure 3.7. We have

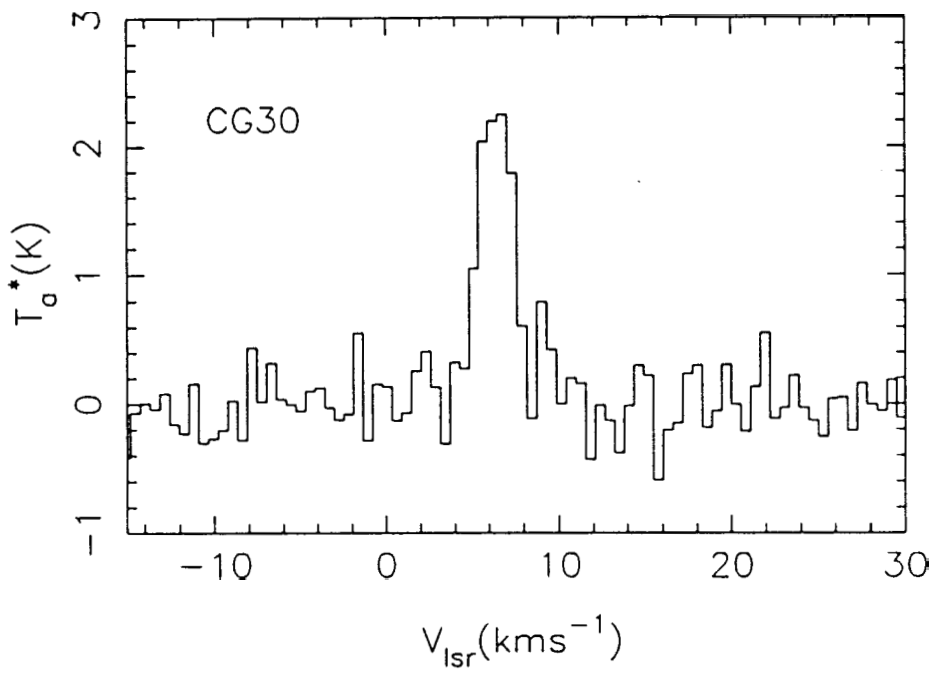

Figure 3.5: A sample ^{12}CO spectrum from observations made during 1989. A fourth order polynomial has been subtracted to remove the baseline curvature due to frequency switching. The back-end was an AOS with 216 kHz resolution.

Table 3.1. 1989 observations.

CG number	$T_a^*(89)$ K	v_{LSR} kms^{-1}	rms K
1	2.3	4.8	0.23
2	2.3	5.4	0.21
3	1.4	0.9	0.34
4	2.1	2.6	0.28
5			0.28
6	1.1	0.9	0.28
7			0.20
8	1.4	−4.9	0.35
10			0.36
13	2.5	4.8	0.21
14	2.3	0.1	0.50
16	1.4	−0.8	0.27
17	0.9	4.8	0.24
18			0.29
22	3.5	7.1	0.37
23			0.31
24	1.3	−11.5	0.23
25			0.34
26			0.16
27	1.5	5.8	0.28
28	0.9	6.5	0.21
29			0.31
30	2.2	5.9	0.22
31	4.9	6.4	0.36
32	0.8	4.8	0.25
33			0.36
36			0.45
37	1.2	7.6	0.25
38			0.21

Note: **a** blank indicates non-detection

Table 3.2. co-ordinates of the cometary globules in the Gum Nebula.

source	co-ordinates (1950.0)												tail length (arc min)	ref.
	head						tail-end							
	RA			DEC			RA			DEC				
	h	m	s	°	′	″	h	m	s	°	′	″		
CG01	7	17	49.7	−44	29	26.2	7	1.5	39.4	−44	29	2	23	M
CG02	7	14	31.3	−43	52	43.8	7	12	49.3	−43	51	24.6	18	M
CG03	7	37	45.9	−47	45	35.1	7	37	26	−47	47	51.4	4	M
CG04	7	32	45.6	−46	50	8.9	i	30	40.5	−46	56	43.2	22	M
CG05	7	39	15.8	−43	42	8.3	7	39	4.6	−43	41	55.1	2	M
CG06	7	29	2.1	−46	37	14.5	i	28	18.9	−46	41	35	9	M
CG07	9	12	26.1	−42	16	54.4	9	13	14.2	−42	18	14.6	9	M
CG08	7	41	1.3	−41	8	32.8	7	40	46.5	−41	S	23.2	3	M
CG09	7	39	7.4	−41	20	4.1	7	38	52.6	−41	19	6.3	3	M
CG10	7	40	55.2	−41	58	11.9	7	40	34.6	1	59	48.4	4	M
CG13	7	12	49.1	−48	23	16.4	7	10	17.6	−48	30	0.2	26	M
CG14	7	37	16.2	−49	1	29.5	7	36	22.4	−49	52	51.8	12	M
CG15	7	31	0.5	−50	39	20.2	i	29	55.2	−50	45	29.1	12	M
CG16	7	26	19.4	−50	58	32.6	7	2.5	47	−51	1	48.7	6	M
CG17	S	51	0	−51	41		S	51	6.5	−51	42	44.4	2	Z
CG18	8	51	0	−50	29		8	51	2.6	−50	30	57.4	2	Z
CG22B1	S	26	48.0	−33	34	12.0	8	27	1 6	−33	14	12	21	S
CG22B2	S	27	16.7	−33	14	12.0	8	28	-1.1	−32	46	11	30	S
CG23	7	34	48	−50	6		7	34	14.6	−50	10	30	7	Z
CG24	8	17	33.0	−42	44	58.4	S	17	14.5	−42	48	45.S	5	M
CG25	7	35	56.0	−47	50	15.1	7	35	19.2	−47	54	47.5	S	M
CG26	8	14	3.3	−33	40	52.8	S	14	12.9	−33	37	36.1	4	M
CG27	8	10	28.4	−33	36	11.6	8	10	33	−33	33	53.6	2	M
CG28	S	10	26.2	−33	46	32.4	S	10	25.8	−33	45	12	1	M
CG29	8	10	27.9	−33	51	54.2	S	10	32.6	−33	49	36.1	3	M
CG30	S	7	40	−35	56	2	8	i	13.4	−35	30	34.1	26	R
CG31A	S	7	10	−3.5	52	24	8	6	36.9	−35	26	53.2	26	R
CG31B	8	6	55	−35	54	14								R
CG31C	S	6	40	−35	50	44								R
CG31D	S	6	24	−35	52	58								R
CG31E	S	6	21	−35	55	1s								R
CG32A	8	12	28.6	−34	21	8.4	8	12	10.8	−34	8	27.9	13	M
CG32B	S	12	2 2 .	−34	18	58.6	8	12	10.8	−34	8	27.9	11	M

Table **3.2.** continued.

source	co-ordinates (1950.0)												tail length (arc min)	ref.
	head						tail-end							
	RA			DEC			RA			DEC				
	h	m	s	°	′	″	h	m	s	°	′	″		
CG33	8	13	33.7	−33	55	19.4	8	13	40.3	−33	52	39	**3**	**M**
CG34	7	27	54	−41	4		7	27	19	−40	57	24	9.4	Z
CG36	8	35	22.7	−36	27	23.9	8	***35***	46.5	−36	22	47.1	7	M
CG37	8	10	29.4	−32	56	21.7	8	10	30.8	−32	52	25.1	4	M
CG38	8	7	47	−36	1	42								R
GDC1	8	24	17	−50	52	5								R
GDC2	8	25	10	−50	51	42								R
GDC3	8	24	56	−50	41	13								R
GDC4	8	25	2	−50	29	53								R
GDC5	8	26	1	−51	0	2								R
GDC6	8	30	30	−50	22	46								R
GDC7	8	32	**39**	−50	S	21								R

References:

Z: Zealey *et. al.*, 1983

R: Reipurth, 1983

S: Sahu ef. *al.*, 1988

M: Our measurements from ESO plates.

Notes:

1. For CGs 31B,C,D,E and 38 tail co-ordinates are not available.
2. The Gum Dark Clouds (GDCs) have been included for completeness.

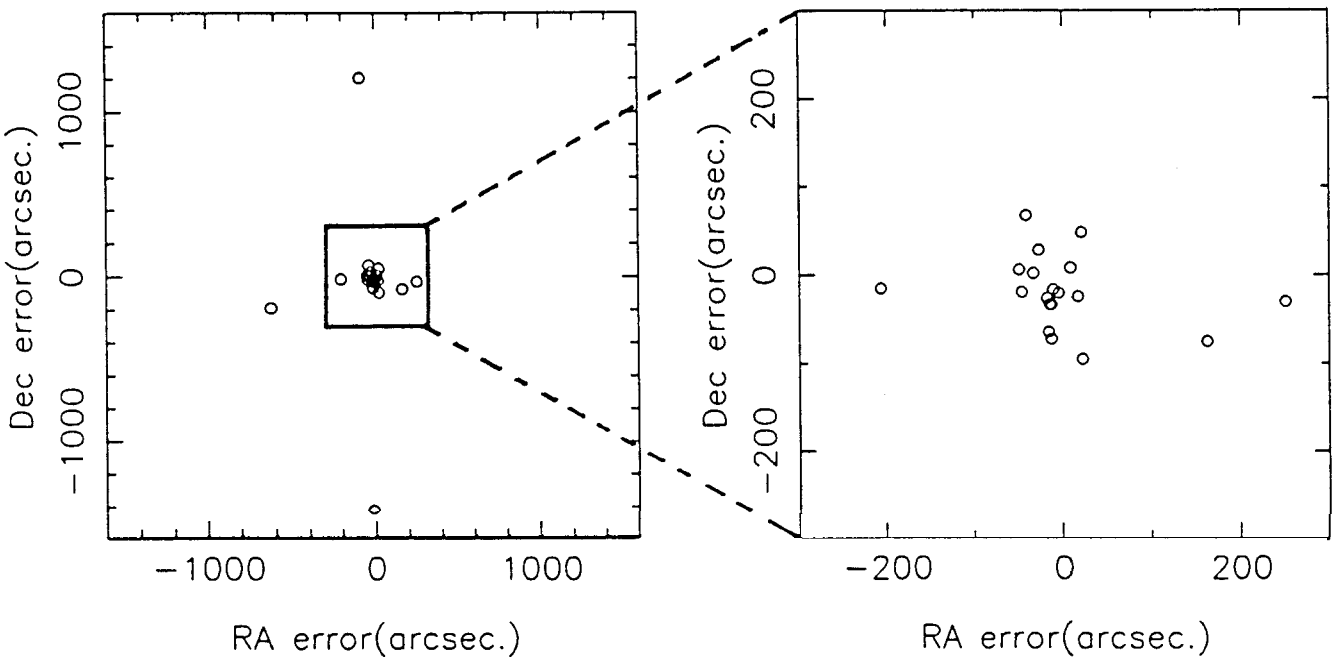

Figure 3.6: Distribution of the errors in the co-ordinates of the CGs. The *error* is defined as the difference between the co-ordinate obtained from literature and that measured from SERC plates.

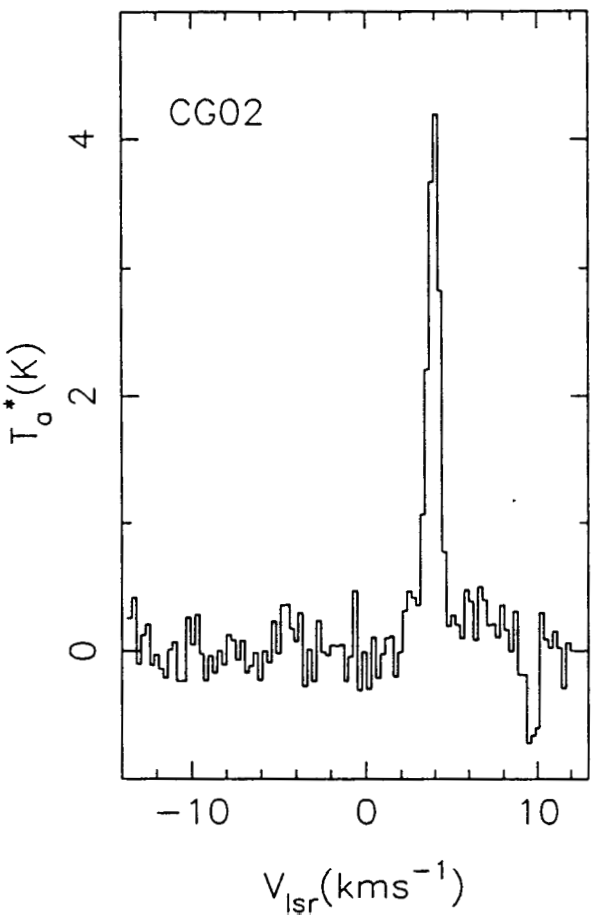

Figure **3.7:** A sample ^{12}CO spectrum from observations made during 1990-91. A fourth order polynomial has been subtracted to remove the baseline curvature due to frequency switching. The back-end was an AOS with 100 kHz resolution.

listed in Table 3.3 the noise levels, measured antenna temperatures and the LSR velocity found by fitting gaussians to the lines from the heads of the CGs. These observations are interpreted in Chapter 4.

3.6 Detection statistics

To establish the reason for non-detections during the previous run, we have plotted in figure 3.8, a histogram of the number of detections and non-detections in the 1989 observations as a function of the co-ordinate errors (defined as the co-ordinates used in the first run *minus* measured co-ordinates used in the second run). Those CGs having large headsizes (CGs 1,2,4,6,22 and 30) have been excluded from the histogram because the errors will not affect their detection. Those CGs for which co-ordinates were not remeasured have also been excluded. It is seen from figure 3.8 that there are no detections if the error is larger than 1'. The four non-detections with error $< 1'$ are CGs with small head sizes ($< 1'$) for which the effect of even small errors and beam dilution are important.

We therefore conclude that the primary cause for non-detections during the first run was the use of wrong co-ordinates.

3.7 Observations of tails

Typically, four points were observed along tlie tails for 21 CGs. The observation procedure was the same as for tlie heads. The points observed were spaced equally along the tails. These observations are summarised in table **3.4.** The velocities, widths and line strengths were obtained by fitting gaussians to the lines. A part of Chapter 4 is devoted to a discussion of these observations.

3.8 Mapping of CG22

The head of the globule CG22, and a part of its tail were mapped in ^{12}CO and ^{13}CO with a grid spacing of 1' both in RA and DEC. Most of the grid points were observed twice and were cornpared for consistency before averaging. In addition, the center point of the grid was observed every day to ensure uniform calibration. These observations were made with a filter bank back-end of 250 kHz resolution. After

Table 3.3. 1990-91 observations.

source	T_a^* K	v_{LSR} kms^{-1}	v_{FWHM} kms^{-1}	rms K
CGO1	5.3	3.3	1.4	0.33
CG02	4.2	4.1	0.9	0.22
CG03	3.3	0.1	1	0.32
CGO4	1.2	1.7	1.2	0.25
CG06	2.9	0.9	1.1	0.26
CG07	5.2	−1.1	0.6	0.54
CGOS	1.7	−5.8	1	0.2
CG09	3.9	−4.2	1.3	0.59
CG10	3.9	−5.5	1.0	0.19
CG13	3.7	3.7	0.8	0.41
CG14	3.0	−0.9	1	0.28
CG15	3.6	−0.8	0.6	0.57
CG16	2.9	−0.7	0.7	0.22
CG17	0.8	3.7	0.8	0.33
CG18	1.0	2.0	0.4	0.26
CG22B1	6.4	6.5	1.1	0.41
CG22B2	6.8	6.8	1.3	0.28
CG22B3	3.4	6.4	1.4	0.22
CG24	2.9	−12.5	1.2	0.2
CG25	2.2	−1.8	0.8	0.29
CG26	3.5	2.0	1	0.51
CG27	2.8	5.0	0.8	0.44
CG28	2.9	5.2	1.1	0.54
CG29	2.4	5.2	0.7	0.31
CG30	3.8	5.8	2.2	0.25
CG31A	4.5	6.0	1.3	0.44
CG31B	4.2	6.0	1	0.36
CG31C	6.8	6.3	1.6	0.3
CG31D	1.5	6.9	1.6	0.29
CG32A	4.5	4.9	1.2	0.43
CG32B	4.7	4.S	1	0.38
CG33	2.3	1.6	0.6	0.46
CG36	1.4	−8.5	0.7	0.39
CG37	3.0	6.2	0.4	0.48
CG38	1.7	7.0	1.2	0.23
GDC1	5.6	5.3	1.3	0.36
GDC2	5.1	6.0	1.4	0.36
GDC3	1.9	5.9	1.0	0.43
GDC4	3.1	4.9	1.3	0.52

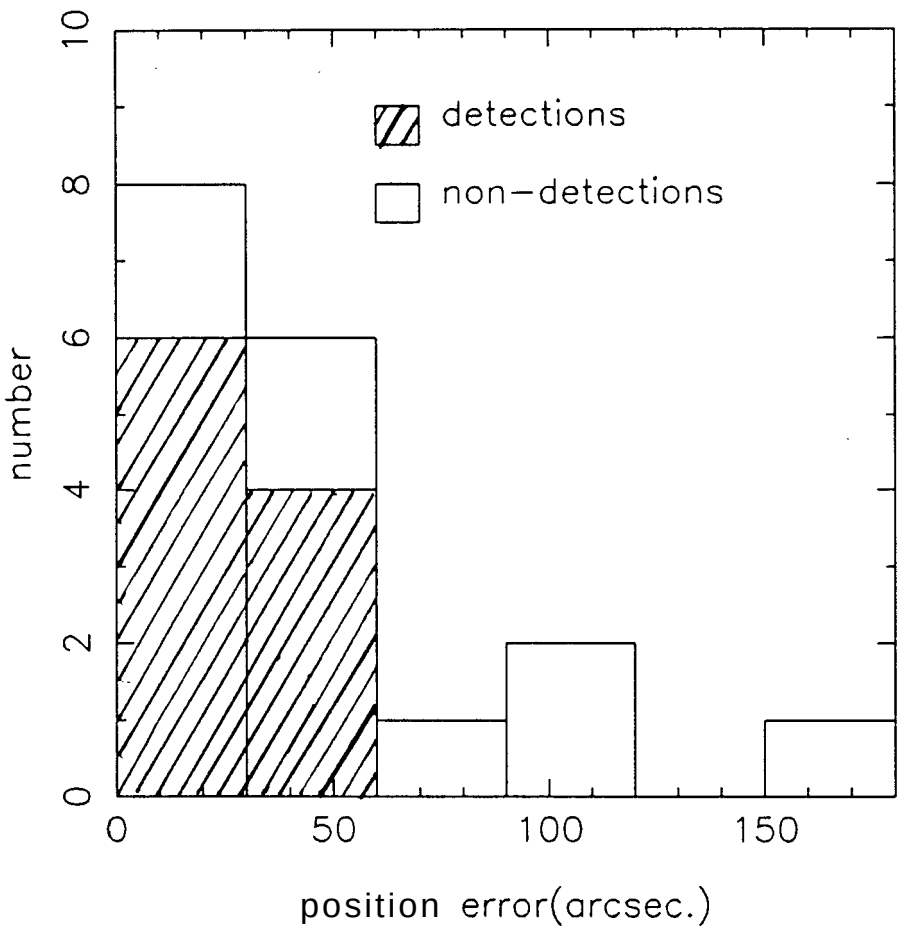

Figure **3.S: A** histogram showing the number of detections and non-detections in the observations done in 1989.

Table 3.4. observations of the tails.

source	T_a^* K	v_{LSR} kms^{-1}	v_{FWHM} kms^{-1}	rms K	distance from head in arcmin
CG1H	5.3	3.3	1.4	0.33	0.0
CG1T2	4.0	3.7	1.1	0.55	14.2
CG1T3	4.2	3.7	1.4	0.39	21.2
CG1T4	4.3	3.4	1.4	0.43	7.0
CG2H	4.2	4.1	0.9	0.24	0.0
CG2T1	1.0	5.1	0.6	0.19	25.3
CG2T3	1.5	4.9	0.9	0.28	19.1
CG2T4	3.4	4.5	1.4	0.41	6.5
CG3H	3.3	0.0	0.9	0.33	0.0
CG3T2	2.0	0.1	0.9	0.32	2.1
CG3T3	2.6	0.1	0.8	0.37	3.2
CG3T4	4.3	0.3	1.1	0.36	1.0
CG4H	1.2	1.7	1.2	0.23	0.0
CG4T1	4.9	1.9	1.2	0.49	17.4
CG4T2	5.6	1.3	1.5	0.43	8.7
CG4T3	5.3	1.7	1.3	0.50	13.0
CGGH	2.9	0.9	1.1	0.26	0.0
CG6T1	1.7	1.6	1.5	0.22	10.9
CG6T2	1.5	0.8	0.8	0.20	5.4
CG6T3	1.0	0.9	1.1	0.21	8.1
CG6T4	3.5	0.8	1.0	0.35	2.7
CG7H	5.4	−1.1	0.6	0.54	0.0
CG7T2	4.1	−1.3	0.7	0.51	1.0
CG7T3	2.4	−1.3	0.9	0.43	1.4
CG7T4	5.4	−1.2	0.8	0.25	0.5
CG9H	2.7	−4.1	1.1	0.20	0.0
CG9T2	4.1	−4.1	1.0	0.45	1.6
CG9T3	3.3	−3.8	1.1	0.32	2.5
CG9T4	3.5	−3.9	1.1	0.32	0.9

Table 3.4. continued.

source	T_a^* K	v_{LSR} kms^{-1}	v_{FWHM} kms^{-1}	rms K	distance from head in arcmin
CG10T2	5.8	−4.7	2.0	0.48	1.4
CG10T3	5.9	−4.5	1.9	0.36	2.0
CG10T4	4.4	−4.4	2.0	0.33	0.7
CG14H	3.0	−0.8	1.0	0.28	0.0
CG14T2	1.5	−0.9	1.0	0.44	7.4
CG14T3	4.6	−1.0	0.7	1.37	11.3
CG15H	3.6	−0.8	0.5	0.58	0.0
CG15T2	3.6	−0.8	0.8	0.52	8.1
CG15T4	3.8	−0.7	0.9	0.34	4.0
CG16H	3.1	−0.7	0.8	0.20	0.0
CG16T1	1.3	−0.8	1.0	0.17	6.6
CG16T2	3.9	−0.7	1.1	0.53	3.4
CG16T3	2.7	−0.8	1.0	0.52	5.0
CG24H	2.9	−12.4	1.14	0.19	0.0
CG24T1	0.3	−12.4	2.14	0.15	4.2
CG24T2	0.6	−12.0	2.00	0.21	2.1
CG24T4	2.9	−12.0	1.20	0.44	1.0
CG26H	2.5	2.1	0.9	0.18	0.0
CG26T1	1.7	2.2	1.0	0.24	3.5
CG26T3	2.3	2.2	0.9	0.18	2.6
CG26T4	4.6	2.2	0.9	0.41	0.9
CG27H	2.0	5.2	0.7	0.25	0.0
CG27T2	4.2	5.1	0.7	0.40	1.2
CG27T3	2.5	5.2	0.8	0.37	1.8
CG27T4	2.5	5.1	0.8	0.29	0.6
CG29H	2.4	5.2	0.7	0.30	0.0
CG29T1	2.6	5.3	0.7	0.24	2.5
CG29T3	1.7	5.2	0.8	0.18	1.9

Table 3.4. continued.

source	T_A^* K	v_{LSR} kms^{-1}	v_{FWHM} kms^{-1}	rms K	distance from head in arcmin
CG31A	4.5	6.0	1.3	0.42	0.0
CG31AT1	1.7	6.9	1.9	0.22	25.3
CG31AT2	3.8	6.3	1.9	0.15	12.6
CG31AT3	3.5	6.6	1.8	0.14	19.0
CG32AT2	2.5	5.2	1.2	0.39	7.7
CG32AT3	4.9	5.5	1.4	0.35	10.5
CG32AT4	6.6	5.0	1.0	0.36	3.8
CG32AH	4.5	4.9	1.2	0.43	0.0
CG32BH	4.7	4.8	1.0	0.38	0.0
CG32BT2	3.8	5.4	1.0	0.41	5.5
CG32BT4	3.0	4.8	1.4	0.41	2.7
CG33H	2.4	1.6	0.5	0.45	0.0
CG33T1	1.6	1.9	0.5	0.35	3.0
CG33T2	3.1	1.8	0.7	0.43	1.6
CG33T3	2.0	1.8	0.6	0.24	2.2
CG33T4	2.3	1.8	0.5	0.51	0.7
CG36H	3.1	10.4	0.7	0.35	0.0
CG36T2	2.8	10.7	0.9	0.35	2.4
CG36T4	4.2	10.6	1.1	0.40	1.2
CG37H	3.0	6.7	0.4	0.46	0.0
CG37T3	1.0	6.8	0.6	0.22	2.9
CG37T4	2.0	6.9	0.8	0.20	1.0

Note: CG33H, for expample, refers to the head of the globule CG33. Similarly. T refers to the tail. T4,T2,T3,T1 represent the sequence of points along the tails moving away from the head. The numbers in parenthesis are estimated errors in the velocity gradients(see text).

initial data reduction using POPS, the maps were made on AIPS. These observations are interpreted in Chapter 5.

3.9 Comparison with other observations

From the observations described above, we have radial velocities for all CGs except CG23 and CG34 which were not detected. The radial velocities were obtained as the *center velocity of the best fitting gaussian to the lines.* As CG10 and CG30 show two components, we take the velocity of the stronger component.

The Columbia CO survey of the third galactic quadrant (May *et al.*, 1988) covered a part of the region over which the CGs are distributed. Since this survey was done with 0.5° resolution we do not expect to see the small CGs because of beam dilution. But any large scale distribution of CO along lines of sight to the CGs *will* show up. We can use these to check if our detections are contaminated by molecular gas not associated with the CGs. We see from the published survey data that CGs 1-6,8-10,13-16 and 25 are *outside* the region covered in the Columbia survey. This, therefore, leaves one with some uncertainty. But the CGs 1-4,6,13-16 and 25 have $b < -12°$ and so their detections are unlikely to be confused by more widespread gas. CGs 5,8,9 and 10 have $b \sim -9°$ and have nearby dark clouds distributed over larger spatial scales. These dark clouds show signs of being affected by ζ Pup and γ^2 Vel. These four CGs show more or less the same radial velocities. All the other CGs are in a region covered by the survey. The GDC complex of which GDCs 1 and 2 show CG features is extended consisting of 7 clouds and has been detected by the survey. The velocities are consistent. Similarly, the CG 30-31 complex, which is extended with more dark clouds in the same region, and the largest globule CG 22, have been detected by the survey with velocities consistent with our values. All other CGs which are small and isolated have not been detected. The survey detected strong CO emission from what is called the Vela Molecular Ridge (VMR), but it has been shown that this emission arises from GMCs at distances 800-2400 pc (Murphy, 1985).

A comparison of our velocities with those of Z83 shows general agreement, except for CG17 for which we measure a velocity of $+3.7$ kms^{-1} as against the value of -6.5 kms^{-1} due to Z83. The radial velocity we measure for CG18 ($\approx 1°$ away from CG17) is $+2.0$ kms^{-1}. The velocities of the clouds in the GDC1-7 complex which is nearby are again in the range $+5$ to $+6$ kms^{-1}. GDC1 and GDC2 have a windswept appearance with tail-like structures pointing in the same general direction as the other CGs and bright rims facing the center. The rough agreement between the

velocities of CG17, CG18 arid the GDCs suggests that the value reported by 283 for CG17 may be in error. As they have not published their spectra, nor mentioned their S/N, we are not in a position to comment any further.

From the above it seems clear that the radial velocities we have obtained are reliable and do nof suffer from contamination from other line of sight material. In addition, thc fact that the 1989 observations using co-ordinates with errors resulted in a lower detection rate supports this conclusion.

REFERENCES

Feitzinger, J.V., Stuwe, J.A. 1984, Asti-on. *Astrophys. Suppl.*, 58, 365.

Hartley, M., Manchester, R.R., Smith, R.M., Tritton, S.B., Goss, W.M. 1986, *Astron. Astrophys. Suppl.*, **63,** 27.

Hawarden, T.G., Brand, P.W.J.L. 1976, *Monthly Notices* Roy. Astron. *Soc.*, 175, 191.

May, J.,Murphy, D.C., Thaddeus, P. 1988, Astron. *Astrophys. Suppl.*, 73, 51.

Murphy, D.C. 198.5, Ph.D. Thesis, Massachusetts Institute of Technology.

Patel, N.A. 1989, Ph.D. Thesis, Indian Institute of Science, Bangalore.

Reipurth, B. 1983, Astron. *Astrophys.*, 117, 183.

Sandqvist, Aa. 1976,*Monthly Notices* Roy. Astron. *Soc.*, 177, 69P.

SAO Star Catalog, 1966 (Smithsonian Institution, Washington, D.C.).

Zealey, W.J., Ninkov, Z., Rice, E., Hartley, M., Tritton, S.B. 1983, *Ap.* Letters, 23, 119(Z83).